

# Remarks on Emotion Recognition Using Breath Gas Sensing System

Kazuhiko Takahashi and Iwao Sugimoto

**Abstract** This paper proposes a smart gas sensing system to achieve emotion recognition using breath gas information. A breath gas sensing system is designed by using a quartz crystal resonator with a plasma-polymer film as a sensor. For computational experiment of emotion recognition, the machine learning-based approaches, such as neural network (NN) and support vector machine(SVM), are investigated. In emotion recognition experiments by using gathered breath gas data under psychological experiments, the obtained maximum average emotion recognition rates are 75% using ANN and 83% using SVM for three emotions: pleasure, displeasure, and no emotion. Experimental results show that using breath gas information is feasible and the machine learning-based approach is well suited for this task.

**Keywords** Emotion · breath gas · quartz crystal resonator · plasma-polymer film · neural network · support vector machine

## 1 Introduction

Emotion recognition is an interesting but difficult task. People can recognize emotional speeches with about 60% accuracy and emotional facial expressions with about 70–98% [1]. Studies on emotion recognition with computers differ on the number of categories and the kinds of categories to use. Some emotion recognition systems in speech or facial expressions which have been used include several emotional states such as joy, teasing, fear, sadness, disgust, anger, surprise, and neutral. In those studies, emotions that are consciously and purposefully expressed by the subjects are treated since consciously expressed emotions are easier to recognize,

---

Kazuhiko Takahashi

Department of Information Systems Design, Doshisha University, Kyoto, Japan,  
e-mail: katakaha@mail.doshisha.ac.jp

Iwao Sugimoto

School of Bionics, Tokyo University of Technology, Tokyo, Japan,  
e-mail: sugimoto@cc.teu.ac.jp

control and significantly to gather data on, however recognition rates are 50–60% in emotional speech recognition [2, 3] and 80–90% in facial expressions [4, 5]. Physiological indexes are also useful to evaluate emotions since they can be measured physically and objectively and can be easily applied to engineering approaches. Physiological changes according to exciting emotions can be observed on changes of the body surface and/or autonomic nervous system [1]: e.g., skin conductivity, electrocardiogram, electromyogram, and blood volume pressure. Using brain waves seems to be effective [6, 7] since emotions are excited in the limbic system and are deeply related to cognition process. In these cases, however, sensors have to be attached to the human body to collect physiological data and expert techniques of handling the sensors are also required. On the other hand, it might be considered that there is a relationship between mental states such as emotion and stress, and physical states of the internal organs or the oral cavity. Since feeling emotions affect the autonomic nervous system, studies of a relevance between breathing patterns and emotions have been carried out [8]. From a viewpoint of relevance between illness and emotions such as a laughter and stress [9], it is shown that changes of the autonomic nervous system based on feeling emotions affect physical states of the internal organs recently. In the field of remoteness medical care, tele-medicine, and tele-care, studies on a disease diagnosis by breath gas test [10, 11, 12, 13] have been carried out actively since it is clear that internal organs disease on a liver, lungs, and blood has bad breath (chemical features) from experience and an analytic chemistry point. As the breath gas test is a non-invasive method of biomarkers without pain, it protects the human body off from the risks of inserting electrodes or sensors. Thus, in a medical field, the breath gas test is expected as diagnosis technology to inspect an internal change of human body. On the other hand, oriental medicine explains the relationship between emotions and internal organs by using five elements (water, fire, wood, metal, and earth) theory of traditional Chinese philosophy as shown in Table 1: liver vs anger, heart vs joy, spleen vs worry, lungs vs sadness, and kidney vs fear. Although it is not commonly guaranteed that there exists such a relationship clearly yet, it might be possible to estimate emotions by using information of internal organs' states indicated by breath gas indirectly. Furthermore, if an evaluation method of mental states by using change of breath gas states can be achieved, information from the breath gas might provide a new man-machine interface. However,

**Table 1** Five elements of Chinese philosophy and biogas components of disease

Five elements	Five organs	Five emotions	Disease	Biogas components
Wood	Liver	Anger	Liver disease, Cirrhosis, Hyper- cholesterolemia	Ammonia, Isoprene, Volatile amines, Volatile sulfur compounds
Fire	Heart	Joy	Myocardial infarction	Pentane
Earth	Spleen	Worry	Diabetes mellitus	Acetone
Metal	Lungs	Sadness	Asthma	Carbon Monoxide
Water	Kidney	Fear	Renal failure	Volatile amines

to date, few study of estimating mental states such as emotions from breath gas information has been undertaken. Therefore, we assume that emotions affect changes in the components of breath gas and investigate a possibility of using biogas emitted from a human body as a new channel of estimating human emotions.

In this paper, we propose a smart gas sensing system for breath gas test and investigate emotion recognition by using machine learning-based approach as a first step to achieve emotion recognition from breath gas information. In Sect. 2, the basic design of breath gas sensing system utilizing a quartz crystal resonator sensor that is a type of mass transducer is described. In Sect. 3, collecting breath gas data using the sensing system under psychological experiments is carried out and some results of computational emotion recognition are presented.

## 2 Breath Gas Sensing System

Figure 1 shows a block diagram of the breath gas sensing system that consists of a sensor module, a power supply, and a personal computer. The sensor module utilized a sensitive sensor device based on a quartz crystal resonator (QCR) with a plasma-polymer film (PPF) where the sensor device can detect volatile organic compounds (VOCs) with parts-per-billion (ppb) levels under the dry air conditions [14, 15, 16]. The PPF was prepared by radio-frequency (RF) sputtering with an organic solid target, which was suitable for mass production and needed no reactive or toxic reagents for processing. A 9 MHz AT-cut QCR, which is 8.5 mm diameter and 0.1 mm thick, was used. As shown in Table 2, the PPFs with different chemical structures were prepared by using various target materials including biomaterials (s1 ~ s5) and synthetic polymers (s6 ~ s7). The electrode's area of the sensor device was 0.13 cm<sup>2</sup>. The relationship between the frequency shift of the QCR  $\Delta f$  (Hz) and mass variation of the organic thin film  $\Delta m$  (ng) is defined with Sauerbrey equation:

$$\Delta m = -1.05\Delta f \quad (1)$$

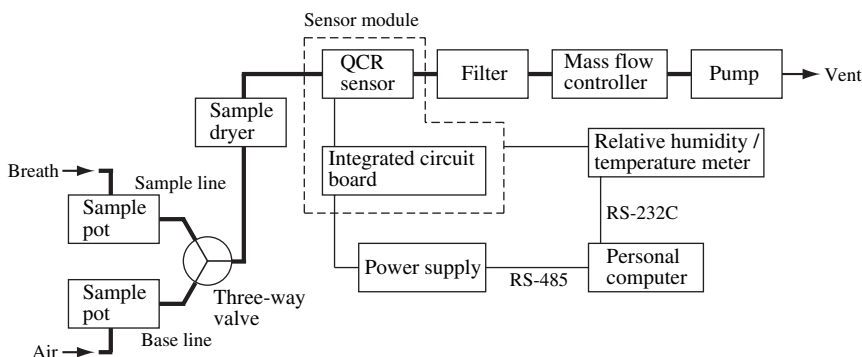


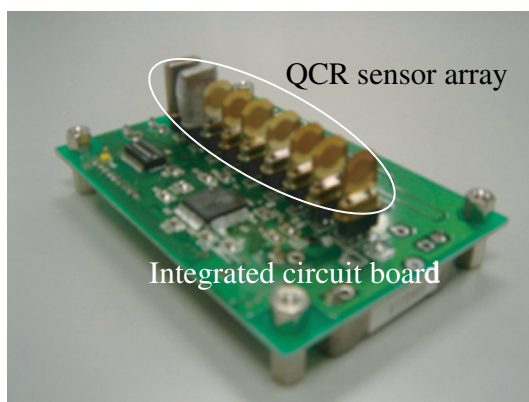
**Fig. 1** Diagram of breath gas sensing system

**Table 2** Materials for organic thin film of sensor cell

Sensor cell	Material
s1	D-phenylalanine
s2	D-tyrosine
s3	D-glucose
s4	DL-histidine
s5	Adenine
s6	Polyethylene (PE)
s7	Polychlorotrifluoroethylene (PCTFE)
s8	D-phenylalanine (Sealing)

The PPF-QCRs were placed in a flow sensor cell and simultaneously attached to an integrated circuit board equipped with a custom LSI for oscillation and resonant frequency measurements and a multiport serial interface as shown in Fig. 2. This sensor module can mount eight PPF-QCRs.

The sensor module was placed in a freeze sealing case. The relative humidity and temperature in the case were measured by a humidity sensor (HMT337, Vaisala, Finland, accuracy:  $\pm 1.0\%$  for 0 to 90% relative humidity). As shown in Figure 1, the breath measurement system consisted of two gas flow lines: a sample line carries breath gas and a reference line carries base gas. In our sensing system, air in indoor atmospheric condition was used as a reference or cleaning gas for establishing the initial state of the QCR sensors. These flow lines were switched by a three-way valve to connect with the gas line of the sensor cell. A sample dryer (Desiccant/Membrane gas dryer DM-110-24, Perma Pure, U.S.A.) was inserted between the valve and the sensor module to dehumidify gas. The flow rates of all flow lines were controlled around 300 mL/min generally by a mass flow controller (SEC-E40MK3, HORIBASTEC, Japan, accuracy:  $\pm 1.0\%$  F.S., control range: 2 ~ 100% F.S., flow range: 10/20/50/100/200/500 SCCM 1/2/3/5/10 SLM) and a dry vacuum pump (Linicon LV-125, NITTO-KOHKI, attainment vacuum level:  $-33.3$  kPa,

**Fig. 2** Configuration of sensor module

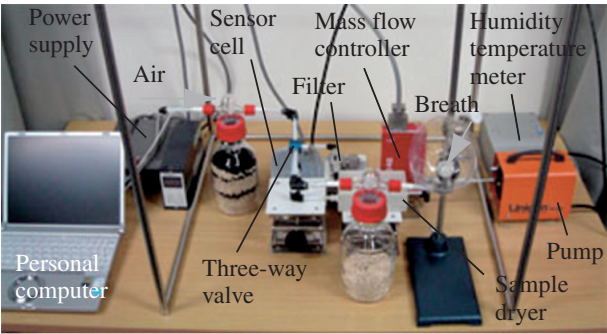


**Fig. 3** Experimental setup

exhalation: 5 L/min). To remove minuteness mist in the gas line, an inline filter (FT4-5, GL Science, Japan, diameter: 5  $\mu\text{m}$ ) was placed between the sensor module and the mass flow controller.

Figure 3 shows the experimental setup for measuring and analyzing breath gas using arrays of PPF-coated QCRs in the laboratory. As shown in Fig. 3, dehumidification by a molecular sieve and deodorization by a carbon were performed before atmosphere of the room was introduced into the reference line, and a sample pot was used as a buffer before introducing breath gas into the sample line. The molecular sieve was also in the sample pot in order to dehumidify the sample gas. A subject covered her/his mouth with a nose pad and blew breath as shown in Fig. 4. The breath gas was introduced into the sensor cell by switching the three-way valve after the baseline fluctuation had been suppressed to below  $\pm 0.1$  Hz for 1minute. Data were collected at 1-second interval for the QCR sensor array and the relative humidity/temperature sensor.

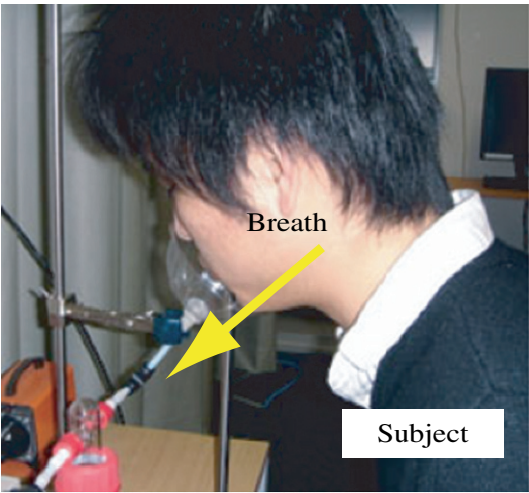
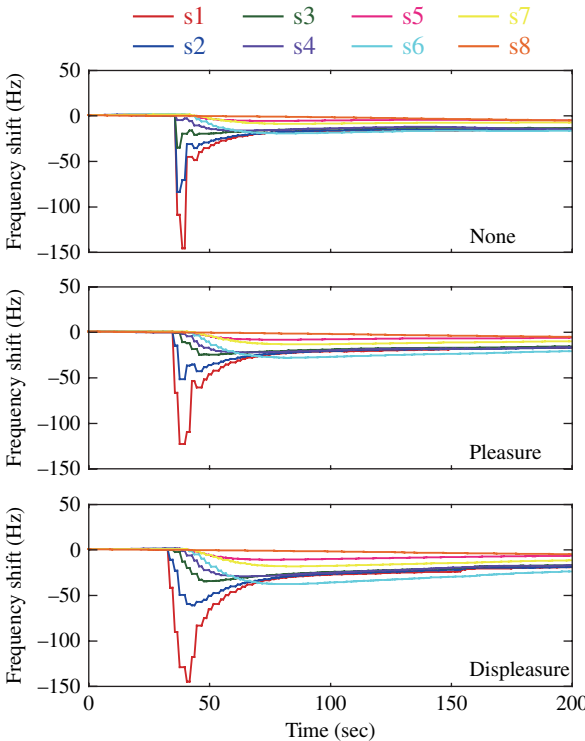


**Fig. 4** Collection of breath gas

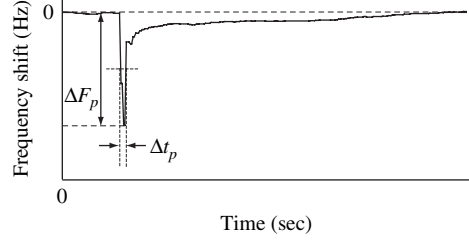
### 3 Experiments of Computational Emotion Recognition

#### 3.1 Recognition of Emotion Elicited by Imaging [17, 18]

The responses of the breath gas sensing system were collected under the psychological experiments. By considering a guide to gathering physiological data for affective recognition described in the affective recognition work [1], the experiments were carried out following an *event-excited, lab setting, feeling, open-recording*, and *emotion-purpose* methodology. In this experiment, three emotions, such as pleasure (positive emotion) and displeasure (negative emotion), and no emotion, were considered. A subject imaged situations of feeling the emotion to excite the emotion, then the subject blew breath into the sample line of the sensing system. The experiment was carried out in our laboratory where the illumination, sounds, and room temperature were controlled to maintain uniformity. The subject was a male, native Japanese and the breath gas was collected four times, one time for each of the three emotions. Figure 5 shows examples of responses from each sensor cell. The horizontal axis is time and the vertical axis is the frequency shift. The subject blew breath to the sample line around 30 seconds, and the flow line was changed into the



**Fig. 5** Examples of responses from breath gas sensing system

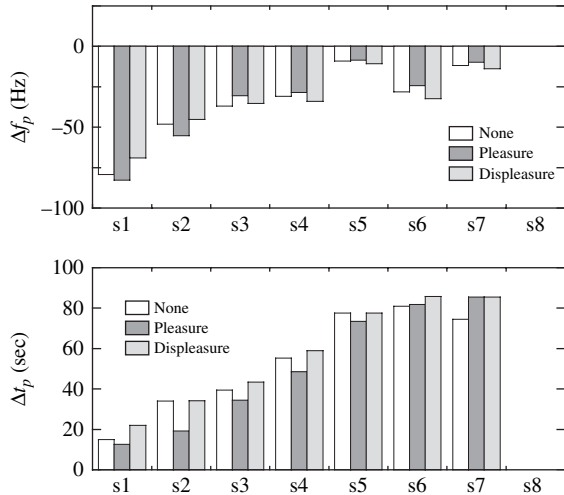
**Fig. 6** Feature extraction

reference line around 90 seconds by the three-way valve. Except for the sensor 8, the response of the frequency shift shows a local minimum after breath introduction and then converges to around zero as shown in Fig. 5. The amplitude of each response curve depends on how strongly the subject blows breath to the sample line, however, the shape of the response curve is not affected.

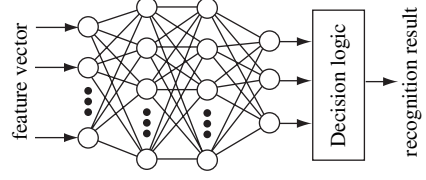
Two features, such as peak  $\Delta f_p$  and pulse width  $\Delta t_p$ , can be extracted from each response curve of sensor. As shown in Fig. 6, the pulse width is defined by the interval that the output of the sensor crosses over the half of the peak. Average value of each feature is calculated by using collected data for every emotional state in every sensor as shown in Fig. 7, but remarkable differences between sensors are not observed by t-test with 5% level of statistical significance. Therefore, the machine learning-based approach is introduced for the emotion recognition task.

The emotion recognition system was composed of artificial neural network (ANN), which is a multi layer feedforward network, and decision logic as shown in Fig. 8. The relationship between inputs and outputs of the ANN is given as follows.

$$y_i = \sum_j w_{3ij} f_j \left\{ \sum_k w_{2jk} f_k \left( \sum_l w_{1kl} x_l \right) \right\} \quad (2)$$

**Fig. 7** Average features under emotional states

**Fig. 8** Artificial neural network-based emotion recognition system



where  $x_l$  is the input to the  $l$ th neuron in the input layer,  $y_i$  is the output of the  $i$ th neuron in the output layer,  $w_{mqr}$  ( $m = 1, 2, 3$ ) is the weight that includes threshold, and  $f(\cdot)$  is a sigmoid function. The learning of the ANN is carried out by the back propagation algorithm to minimize the cost function  $J$  as follows.

$$J = \frac{1}{2} \sum_p \sum_i (y_{d_i} - y_i)^2 \quad (3)$$

$$w_{mqr}(t+1) = w_{mqr}(t) - \eta \frac{\partial J}{\partial w_{mqr}(t)} + \mu \Delta w_{mqr}(t) \quad (4)$$

where  $\eta$  is the learning factor,  $\alpha$  is the momentum factor,  $\Delta w_{mqr}(t)$  is the weight increments at the  $t$ -th iteration,  $y_{d_i}$  is the teaching signal, and  $p$  is the total number of the training data. The learning factors  $\eta$  and  $\mu$  are tuned by the following rules.

$$\eta(t+1) = \begin{cases} (1+\beta)\eta(t) & J(t) < J(t-1) \\ \eta(t) & J(t) = J(t-1) \\ (1-\gamma)\eta(t) & J(t) > J(t-1) \end{cases}$$

$$\mu(t+1) = \mu(t) + \Delta\mu$$

where  $\beta$ ,  $\gamma$ , and  $\Delta\mu$  are positive constant values.

In the experiment, two types of input vector to the ANN were composed of the features extracted from the response curves as follows.

- input vector (a): pulse width  $\Delta t_{p_i}$  ( $i = 1, 2, \dots, 7$ )

$$\mathbf{x} = [\Delta t_{p_1} \ \Delta t_{p_2} \ \dots \ \Delta t_{p_7}]$$

- input vector (b): peak  $\Delta f_{p_i}$  and pulse width  $\Delta t_{p_i}$  ( $i = 1, 2, \dots, 7$ )

$$\mathbf{x} = [\Delta f_{p_1} \ \Delta f_{p_2} \ \dots \ \Delta f_{p_7} \ \Delta t_{p_1} \ \Delta t_{p_2} \ \dots \ \Delta t_{p_7}]$$

The input vector (a) is used only the pulse width information since it is hard to be affected by how to blow the breath. On the other hand, the vector (b) utilizes all features. Because of the difference between the units of two features, each element of the vector (b) is normalized by using mean and standard deviation when it applies to the ANN.



**Table 3** Emotion recognition results using ANN with input vector (a) [%]

In \ Out	Pleasure	Displeasure	None
Pleasure	75.0	25.0	0.0
Displeasure	50.0	25.0	25.0
None	25.0	25.0	50.0

There were 3 neurons in the output layer of the ANN. In the learning process of the ANN, the teaching signals  $y_{d1}y_{d2}y_{d3}$  were defined as follows: the set of [100] indicated displeasure, the set of [001] indicated pleasure, and the set of [010] indicated no emotion. The learning was quitted if the cost function achieved  $10^{-4}$ . In the emotion recognition process, the output from the ANN was investigated in the decision logic that selects the best emotion; the output neuron whose output value closes ‘1’ is chosen, and it indicates the recognition result. The leave-one-out cross-validation method was used to evaluate the recognition ability of ANN.

Table 3 shows the emotion recognition result by using the input vector (a) where a (7-11-11-3) network was used. The number of neuron in the hidden layers and the learning factors were determined by trial and error in order to converge the learning of ANN:  $\eta(0) = 10^{-4}$ ,  $\beta = \gamma = 10^{-5}$ ,  $\mu(0) = 0.1$ , and  $\Delta\mu = 10^{-4}$ . In the tuning of the learning factors, the upper and lower values of  $\eta$  were 0.1 and  $10^{-5}$ , respectively, and upper value of  $\alpha$  was 0.9. Though the recognition rate of 100% is achieved for the teaching data after the learning of ANN is completed, the averaged recognition rate defined with the average of the diagonal element is lower than 50% for the test data. Displeasure and no emotion are hard to recognise correctly. Table 4 shows the emotion recognition result by using the input vector (b) where a (14-14-6-3) network was used. The averaged recognition rate of 75% is achieved, however, misrecognition of pleasure increases.

As an alternative of using the ANN, support vector machine (SVM) was applied to the emotion recognition experiment. The SVM is originally designed for two-class classification and is finding the optimal hyperplane that minimizes the expected classification error of test samples by using statistical learning theory. Given a labelled set of training data  $(\mathbf{x}_i, u_i)$  where  $\mathbf{x}_i$  is input vector ( $\mathbf{x}_i \in R^N$ ) and  $u_i$  is the associated label ( $u_i \in (-1, 1)$ ), the optimal hyperplane  $\mathbf{w}\mathbf{x} + b = 0$  can be found by minimizing  $\|\mathbf{w}\|^2 + C \sum_i \xi_i$  constrained by:  $\xi_i \geq 0$  and  $u_i(\mathbf{w}_i \cdot \mathbf{x} + b) \geq 1 - \xi_i$ . Here  $\xi_i$  is the slack variable that is introduced to account for non-separable data,  $C$  is the margin parameter that quantifies the trade-off between training error and system capacity. Solving the quadratic programming problem, the optimal hyperplane can be defined as follows.

**Table 4** Emotion recognition results using ANN with input vector (b) [%]

In \ Out	Pleasure	Displeasure	None
Pleasure	50.0	50.0	0.0
Displeasure	25.0	75.0	0.0
None	0.0	0.0	100.0

$$g(\mathbf{x}) = \sum_i u_i \alpha_i^* K(\mathbf{x}, \mathbf{x}_i^*) + b^* \quad (5)$$

where  $K(\cdot, \cdot)$  is a kernel function,  $\mathbf{x}_i^*$  is a support vector that corresponds to a nonzero Lagrange multiplier  $\alpha_i^*$ , and  $b^*$  is a bias parameter. While the kernel function is a simple dot product for a linear SVM, a nonlinear function of the kernel function projects the data to high dimensional feature space in a nonlinear SVM and the optimal hyperplane is found in that space. Several kernel functions such as Gaussian and polynomial functions have been used in the nonlinear SVM.

$$K(\mathbf{x}, \mathbf{y}) = \exp(-\gamma \|\mathbf{x} - \mathbf{y}\|^2) \quad (6)$$

$$K(\mathbf{x}, \mathbf{y}) = (\mathbf{x} \cdot \mathbf{y} + 1)^d \quad (7)$$

where  $\gamma$  is spread of a Gaussian cluster and  $d$  is the degree of freedom in a polynomial kernel. To apply the SVM for multiclass classification, the one-vs-all method [19] as shown in Fig. 9 was implemented. Three SVMs that correspond to each of the three emotions were used. In the emotion recognition process, the feature vector was simultaneously fed into all SVMs and the output from each SVM was investigated in the decision logic that selects the best emotion; the class of the SVM indicates the recognition result.

The input vector of the SVMs was the input vector (a). Training and testing of the SVMs were carried out by the leave-one-out cross-validation method. In the SVMs, the 3rd order polynomial function was used as the kernel function and the margin parameter  $C$  was chosen as 1 in the case of the input vector (a) and was set to 10 in the case of the input vector (b). The other parameters were defined by trial and error in order to achieve complete classification rate for training data. Tables 5 and 6 show the emotion recognition result. The averaged recognition rate of 83% is achieved with the input vector (a), while the recognition rate decreases with the input vector (b).

These results indicate that the machine learning technique such as ANN and SVM is suited for the emotion recognition task using breath gas information, but the recognition results are obtained by using only one subject's data. Therefore, the result obtained in this experiment depends greatly on person. More number of sample data should be required in order to evaluate the emotion recognition system in details.

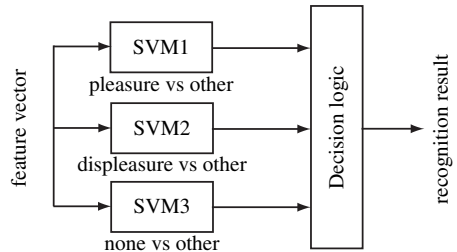


**Fig. 9** SVM-based emotion recognition system

**Table 5** Emotion recognition results using SVM with input vector (a)[%]

In\Out	Pleasure	Displeasure	None
Pleasure	100.0	0.0	0.0
Displeasure	25.0	75.0	0.0
None	25.0	0.0	75.0

**Table 6** Emotion recognition results using SVM with input vector (b)[%]

In\Out	Pleasure	Displeasure	None
Pleasure	50.0	25.0	25.0
Displeasure	50.0	50.0	0.0
None	0.0	50.0	50.0

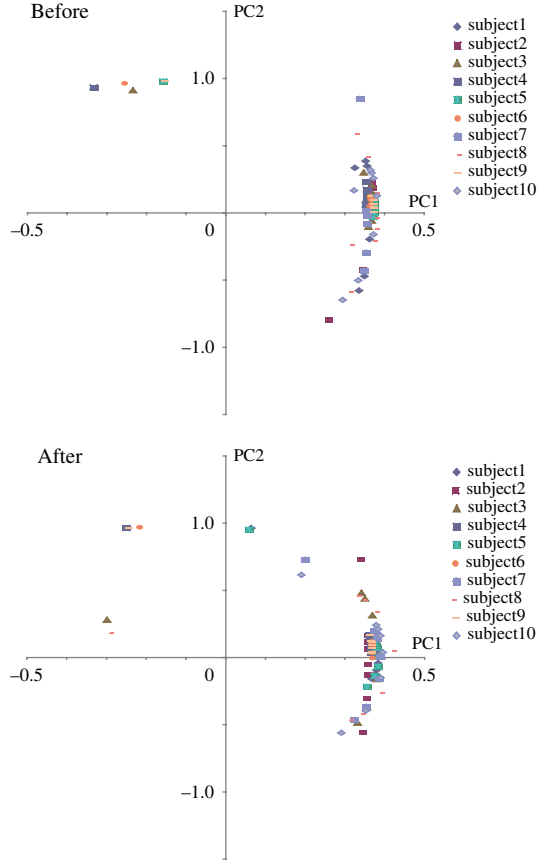
**3.2 Recognition of Emotion Excited with Dental Rinse**

In this experiment, two emotions, such as comfortableness (refreshing emotion) and no emotion, were considered. By using a dental rinse as a stimulus for exciting emotion, the responses of the breath gas sensing system were gathered. The experiments were carried out in our laboratory where the illumination, sounds, and room temperature were controlled to maintain uniformity. The experiments were done by 10 subjects of our laboratory (males, native Japanese). In the experiment, the subject first blew his breath into the gas sensing system under no emotion. After 10 minutes interval, the subject washed his mouth with the dental rinse and then blew his breath into the gas sensing system. The dental rinse is a commercial product (<http://www.teamgum.net/eng/index.html>). The emotions of subjects were evaluated by using questionnaires based on the multiple mood scale [20].

In order to compose input vector of the emotion recognition system, principle component analysis (PCA) is introduced to extract features from each response curve of sensor. The data matrix is defined by using all sensor data that are obtained during the interval of 30 seconds after the flow line was changed into the sample line. The PCA is applied to the data matrix, and two principle components are calculated in the 8 sensors. Figure 10 shows the PCA score plot. The horizontal axis is the first principle component (PC1) while the vertical axis is the second principle component (PC2). The top of Fig. 10 shows the PCA score plot obtained before using dental rinse. The bottom of Fig. 10 shows the PCA score plot obtained after using dental rinse. Here the results of all subjects are illustrated. The distribution of the PC2 is changed after using the dental rinse, however it is very small and depends on the subject.

In the questionnaires, 8 emotions, such as depression/anxiety, hostility, boredom, liveliness, well being, friendliness, concentration, and startle, were investigated before and after using the dental rinse. A semantic profile was utilized to evaluate the questionnaires. The semantic profile shows that the degrees of negative emotions (depression/anxiety, hostility, boredom) decrease while the degrees of positive

**Fig. 10** Score plot of PCA  
(*top*: before using dental  
rinse, *bottom*: after using  
dental rinse)



emotions (liveliness, friendliness, concentration) increase after using the dental rinse. Therefore, we assume that the subject feel comfortableness/refreshing emotion by using the dental rinse.

To achieve computational emotion recognition, the ANN was used in the emotion recognition system. The input vector of the ANN was composed with the first and second principle components of PCA results for all sensors as follows.

$$\mathbf{x} = \begin{bmatrix} PC_1^{s_1} & PC_2^{s_1} & PC_1^{s_2} & PC_2^{s_2} & \dots & PC_1^{s_8} & PC_2^{s_8} \end{bmatrix}$$

where  $PC_i^{s_j}$  is the  $i$ th principle component of the sensor  $j$ . Training and testing of the ANN were carried out by the leave-one-out cross-validation method. Table 7 show the emotion recognition result where a (16-12-8-6-2) network was used. The averaged recognition rate of 70% is achieved. This result shows the feasibility of our emotion recognition system based on the ANN using breath gas information.

**Table 7** Emotion recognition results using ANN [%]

In\Out	None (before)	Refreshing (after)
None (before)	50.0	50.0
Refreshing (after)	10.0	90.0

4 Conclusions

This paper proposed a smart gas sensing system to achieve emotion recognition using breath gas information. A quartz crystal resonator with a plasma-polymer film was used as a sensor, and breath gas sensing system was designed under air in indoor atmospheric condition. The machine learning-based approach was conducted for computational emotion recognition and its characteristics were investigated. Experimental results demonstrated that using breath gas information is feasible and that the machine learning-based approach such as artificial neural network and support vector machine is well suited for this task.

There are many works to be done in the emotion recognition from breath gas information. In the sensing system, stabilization of the reference is required since the reference is easily affected from the air condition of the room. Improving how to introduce breath gas into the sensing-system is also important. Possible features of breath gas have to be selected in the feature extraction process, and further trials with different recognition methods may help improve recognition performance.

**Acknowledgements** This work was supported by JSPS Grant-in-Aid for Scientific Research (C) 18500142.

References

1. Picard R W, Vyzas E, Healey J (2001) Toward Machine Emotional Intelligence: Analysis of Affective Physiological State. *IEEE Transactions on Pattern Analysis and Machine Intelligence*, 23(2):1175–1191
2. Dellaert F, Polzin T, Waibel A (1996) Recognizing Emotion in Speech. In: *Proceedings of Fourth IEEE International Conference on Spoken Language Processing*, 3, Philadelphia, U.S.A., pp 1970–1973
3. Nicolson J, Takahashi K, Nakatsu R (2000) Emotion Recognizing in Speech Using Neural Networks. *Neural Computing and Applications*, 9(4):290–296
4. Essa I A, Pentland A P (1995) Facial Expression Recognition using a Dynamic Model and Motion Energy. In: *Proceedings of International Conference on Computer Vision*, Cambridge, U.S.A., pp 360–367
5. Yacoob Y, Davis L (1996) Recognizing Human Facial Expressions from Log Image Sequences Using Optical Flow. *IEEE Transactions on Pattern Analysis and Machine Intelligence*, 18(6):636–642

6. Ishino K, Hagiwara M (2003) A Feeling Estimation System Using a Simple Electroencephalograph. In: Proceedings of 2003 IEEE International Conference on Systems, Man, and Cybernetics, Washington, D.C., U.S.A., pp 4204–4209
7. Takahashi K (2005) Remarks on Emotion Recognition from Multi-Modal Bio-Potential Signals. *The Japanese Journal of Ergonomics*, 41(4):248–253
8. Masaoka Y, Honma I (2004) The Effect of Pleasant and Unpleasant Odors on Levels of Anticipatory Anxiety: Analysis Observing Respiratory Patterns. *AROMA RESEARCH*, 5(1):44–49
9. Yoshino S, Kurai T (2001) A Laughter and Immunity. *Journal of Clinical and Experimental Medicine*, 197(12):916–917
10. Dubowski K M (1974) Breath Analysis as a Technique in Clinical Chemistry. *Clinical Chemistry*, 20:966–972
11. Manolis A (1983) The Diagnostic Potential of Breath Gas. *Clinical Chemistry*, 29:5–15
12. Phillips M (1992) Breath Tests in Medicine. *Scientific American*, 267:74–79
13. Yatagai M, Kawasaki M (2003) *AROMA SCIENCE Series 21(4)*. FRAGRANCE JOURNAL Ltd., Tokyo
14. Sugimoto I, Nakamura M, Ogawa S, Seyama M, Katoh T (2000) Petroleum Pollution Sensing at Ppb Level Using Quartz Crystal Resonators Sputtered with Porous Polyethylene Under Photo-Excitation. *Sensors and Actuators*, B64:216–223
15. Seyama M, Sugimoto I, Miyagi T (2002) Application of an Array Sensor Based on Plasma-Deposited Organic Film Coated Quartz Crystal Resonators to Monitoring Indoor Volatile Compounds. *IEEE Sensors Journal*, 2(5):422–427
16. Sugimoto I, Nagaoka T, Seyama M, Nakamura M, Takahashi K (2007) Classification and Characterization of Atmospheric VOCs Based on Sorption/Desorption Behaviors of Plasma Polymer Films. *Sensors and Actuators*, B124:53–61
17. Takahashi K, Sugimoto I (2007) Neural Network Based Emotion Recognition Using Breath Gas Sensing System. In: Proceedings of the 2nd International Conference on Sensing Technology, Palmerston North, New Zealand, pp 467–472
18. Takahashi K, Sugimoto I (2006) Remarks on Breath Gas Sensing System and Its Application to Man-Machine Interface. In: Proceedings of the 3rd International Conference on Autonomous Robots and Agents, Palmerston North, New Zealand, pp 361–366
19. Chapelle O, Haffner P, Vapnik V (1999) Support Vector Machines for Histogram-based Image Classification. *IEEE Transactions on Neural Networks*, 10(5):1055–1064
20. Terasaki M, Kishimoto Y, Koga A (1992) Construction of a Multiple Mood Scale. *Shinrigaku kenkyu : The Japanese Journal of Psychology*, 62(6):350–356